Post-operative elimination of sevoflurane anesthetic and hexafluoroisopropanol metabolite in exhaled breath: pharmacokinetic models for assessing liver function

PK models of SEV and HFIP elimination in breath

S Ghimenti[1], F Di Francesco[1,4], M Onor[2], M A Stiegel[3], M G Trivella[4], C Comite[5], N Catania[5], R Fuoco[1] and J D Pleil[6]

[1] Dipartimento di Chimica e Chimica Industriale, Università di Pisa, Via del Risorgimento, 35 56126 Pisa, Italia

[2] Istituto di Chimica dei Composti Organometallici, Consiglio Nazionale delle Ricerche, Pisa, Italia

[3] Department of Environmental Sciences and Engineering, School of Public Health, University of North Carolina, Chapel Hill, NC, USA

[4] Istituto di Fisiologia Clinica, Consiglio Nazionale delle Ricerche, Pisa, Italia

[5] Azienda Ospedaliero Universitaria Pisana, Pisa, Italia

[6] Human Exposure and Atmospheric Sciences Division, NERL/ORD, U.S. Environmental Protection Agency, Research Triangle Park, NC, USA

E-mail: fdifra@dcci.unipi.it

Abstract

Sevoflurane (SEV), a commonly used anesthetic agent for invasive surgery, is directly eliminated via exhaled breath and indirectly by metabolic conversion to inorganic fluoride and hexafluoroisopropanol (HFIP), which is also eliminated in the breath. We studied the post-operative elimination of SEV and HFIP of six patients that had undergone a variety of surgeries lasting between 2.5 to 8.5 hours using exhaled breath analysis. A classical three compartments pharmacokinetic model developed for the study of environmental contaminants was fitted to the breath data. We found that SEV kinetic behavior following surgery (for up to 6 days) is consistent across all subjects whereas the production and elimination of HFIP varies to some extent. We developed subject specific parameters for HFIP metabolism and interpreted the differences in the context of timing and dose of anesthesia, type of surgery, and specific host factors. We propose methods for assessing individual patient liver function using SEV as a probe molecule for assessing efficiency of liver metabolism to HFIP. This work is valuable not only for the clinical study of metabolism recovery, but potentially also for the study of the interaction of other manufactured and environmental compounds with human systems biology in controlled exposure and observational studies.

Keywords: sevoflurane, hexafluoroisopropanol, pharmacokinetic models, exhaled breath, liver function

1. Introduction

Post-operative recovery from organ transplant is generally monitored with organ biopsy and/or assessment of specific biomarkers in blood. The recovery of liver function, in particular, can also be assessed by dynamic tests such as the plasma clearance of indocyanine green [1], sulfobromophthaleinand galactose [2] or the monitoring in breath of metabolites of labeled compounds [3,4]. However, all these procedures are invasive for requiring intravenous administration of xenobiotics.

We imagined that sevoflurane (SEV), an anesthetic routinely administered during surgery, may be used as a probe molecule to assess the recovery of liver function after a liver transplant. Liver function could be related to the production of a primary liver metabolite, hexafluoroisopropanol (HFIP), which like SEV can be monitored non-invasively in exhaled breath. In this work, we model the post-operative elimination of SEV and HFIP as a first step in developing a novel test for the liver function.

Anesthetics like SEV, desflurane, and isoflurane, as well as other common exogenous substrates (e.g. ethanol, caffeine) are all metabolized by cytochrome P450 2E1 (CYP2E1) [5,6]. In humans, most (>90%) of CYP2E1 resides in the liver, with the remainder distributed in other organs including brain, kidney, and intestine. For modeling purposes, the extra-hepatic metabolism by CYP2E1 is considered negligible [7], so we assigned any measurable production of HFIP as originating in the liver.

Our predictive mechanism is based on classical pharmacokinetic (PK) models for calculating adsorption, distribution, metabolism, and elimination of exogenous compounds [8,9,10,11,12,13,14,15,16]. We used literature values for SEV and HFIP pharmacokinetics [17] to build and calibrate an incremental model, which was tested against other literature data [18] and then applied to empirical data (SEV and HFIP measurements) and meta-data (duration of surgery, applied SEV concentration) from six patients who received invasive surgeries ranging from 2.5 to 8.5 hrs duration. A series of post-operative breath samples were collected and analyzed for SEV and HFIP and served to validate the original models and to interpret liver function.

SEV (1,1,1,3,3,3-hexafluoro-2-(fluoromethoxy)propane, $C_4H_3F_7O$) is currently one of the most used anesthetics due to its favourable pharmacokinetic properties (i.e. low blood-gas partition coefficient, low tissue solubility, fast metabolism and reduced cardio-depressant effect) [19,20]. The low blood-gas solubility enables a rapid induction of anaesthesia and a rapid recovery at the end.

SEV is quickly eliminated via exhaled breath. Only a limited amount (1-5%) of the absorbed SEV undergoes a biotransformation to organic and inorganic metabolites, principally by CYP2E1 [6]. CYP2E1 catalyzed SEV oxidation produces equimolar amounts of inorganic fluoride and HFIP as the principal by-products [21,22,23]. Once formed, HFIP is rapidly conjugated with glucuronic acid in the liver and

excreted in urine as a glucuronide conjugate. The unconjugated fraction, representing less than 15% of total HFIP concentration [17], is then eliminated via exhaled breath. Unconjugated HFIP and HFIP-glucoronide appear in blood 5 minutes after the beginning of anaesthesia. The peak of HFIP concentration in plasma occurs 2-10 hours after the end of anaesthesia, with an average delay of 5.5 hours in patients receiving an average dose of 3.7 minimal alveolar concentration–hours (MAC-h) [24].

The use of a safe probe molecule such as SEV has broader application than non-invasive clinical diagnosis of liver function; we envision that this approach may be implemented in other *in vivo* systems or for *in vitro* assessments of chemical toxicity using human cell-lines. This approach, wherein a specific molecule is used to develop a mode of action for organ involvement, lays the foundation for future work for exploring human systems biology in more general terms with respect to exposure science and risk assessment [25,26].

2. Materials and Methods

2.1 Empirical data from literature: A

The first data set comprised values from Kharasch et al.[17]. These subjects were nominally healthy non-smokers with normal indexes for liver and renal function who underwent elective surgeries with a 3 hrs SEV anesthesia. Blood concentrations of SEV and HFIP were estimated from graphs and literature [17,27]. They are reported in table 1 using the original units of μM in plasma and the expected concentrations (our estimate) in exhaled breath. For SEV, we used for conversion the accepted value 0.65 for blood/breath partition coefficient [27] and the near body temperature approximation of 24.2 liters/mole of an ideal gas. For HFIP, we first converted the total HFIP measurements into the expected free HFIP partition (see column 3) that is available for pulmonary elimination as discussed by Bordeaux et al. [27]. The blood/breath ratio for HFIP is not available in the literature, however, we estimated it to be 6.0 based on ratios of SEV/HFIP in plasma from Kharasch, compared to SEV/HFIP ratios in breath observed by us. The resultant calculated breath concentrations, expressed as parts per million by volume (ppmv) in air, are given in columns 5 and 6. These approximations serve only as scaling factors and so do not affect the shape of the graphs or the subsequent models.

Table 1. Literature values and unit conversion for SEV uptake and elimination and HFIP produced from Kharasch et al. 1995 and Bourdeaux et al. 2010.

Time (hrs)	SEV blood (µM)	HFIP total blood (µM)	(Estimated) HFIP free blood (µM)	(Approx.) SEV breath (ppmv)	(Approx.) HFIP breath (ppmv)
0	0	0	0	0	0
0.1	400			14892	
1	650	14	2.1	24200	56
2	700	21	3.15	26062	85
3	700	29	4.35	26062	117
4	190	26	3.9	7074	105
5	120	45	6.75	4468	182
6	70	33	4.95	2606	133
7	60	42	6.3	2234	169
9	43	33	4.95	1601	133
11	33	34	5.1	1229	137
12		33	4.95		133
24		23	3.45		93
36		17	2.55		69
48		12	1.8		48
60		7	1.05		28
72		5	0.75		20

2.2 Empirical data from literature: B

A second set of blood data was estimated from graphs and discussions from Yasuda et al. [18] (table 2). These data do not include values for the metabolite HFIP and so are only useful for validating the uptake and elimination kinetics of SEV itself. These researchers administered 1% SEV gas for 30 minutes to seven healthy male volunteers (23 ± 3 yrs). Data are expressed as a ratio of end tidal exhalation and administered concentrations; for consistency with the previous dataset, we converted the data into ppmv in the last column of the table.

Table 2. Literature values and unit conversion for SEV uptake and elimination from Yasuda et al. 1991.

Time (hrs)	SEV Fa/Fi	SEV Fa/Fa0	SEV (ppmv)
0.000	0		0
0.013	0.46		4600
0.017	0.55		5500
0.025	0.64		6400
0.033	0.68		6800
0.050	0.72		7200
0.083	0.75		7500
0.125	0.78		7800
0.167	0.79		7900
0.208	0.8		8000
0.250	0.81		8100
0.333	0.82		8200
0.417	0.835		8350
0.483	0.84		8400
0.517		0.4	3360
0.625		0.1	840
0.833		0.06	504
1.167		0.032	269
1.500		0.02	168
2.000		0.012	101
2.500		0.01	84
24.000		0.007	59

2.3 Conceptual model

We developed a classical pharmacokinetic model based on the approximated breath data from Kharasch et al. [17]. The model, based on a previous work [13], is developed for SEV using three empirical compartments: 1st "central" compartment (blood), 2nd compartment (HPT - highly perfused tissues), and 3rd compartment (PPT - poorly perfused tissues). The metabolite is tracked using one or two compartments as the empirical data dictate; the rate constant K_o is for uptake in units of mass/time, the rate constants labeled as K_i's and those labeled as C_i's are in units of 1/time. The K_i's represent the rates

of internal redistribution and the C_1, C_2 and C_3 represent all unrecovered losses of breath SEV, breath HFIP, and other metabolic conversions, respectively. Furthermore, the rate constants for the various compartments automatically reflect their respective hypothetical volumes of distribution because we have access to experimental concentration data. Blood concentrations are considered directly proportional to breath concentrations under the assumptions of linear kinetics for both SEV and HFIP. The conceptual diagram is shown in figure 1.

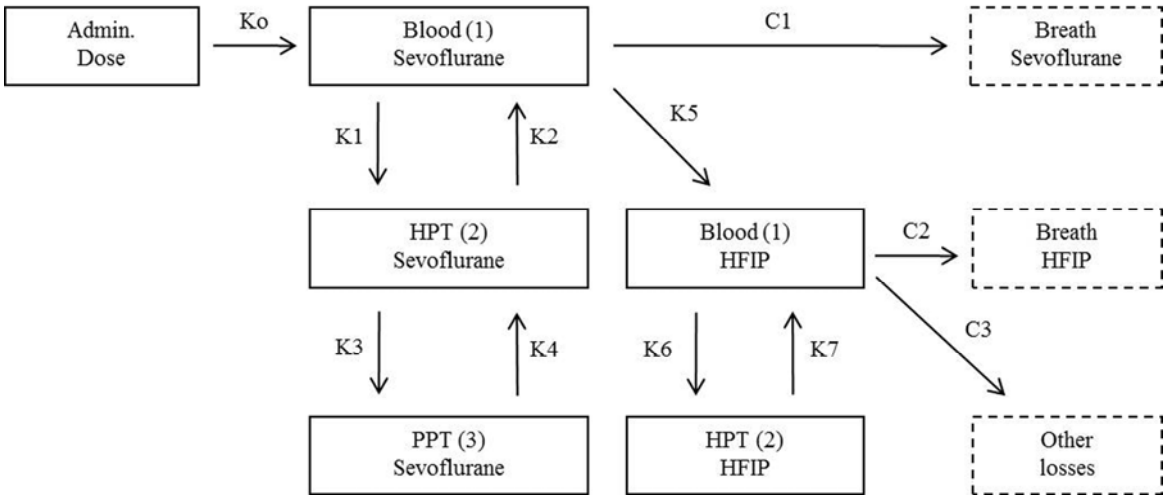

Figure 1. Conceptual model for SEV absorption (administration), distribution, metabolism and elimination. The model assumes linear kinetics and proportional elimination via breath. Annotated arrows represent rate constants and boxes represent concentrations of the respective compounds. C1 and C2 represent losses to breath and C3 represents loss of HFIP to further metabolism and other unknown removal pathways.

2.4 Calculational model

Based on the concepts of linear kinetics and the diagram in figure 1, we write difference equations to calculate the concentrations in each of the compartments as an incremental function of time:

$$C_{blood_{Sev}}(t+\Delta t) = C_{blood_{Sev}}(t) + \Delta t \cdot (C_a \cdot K_0) - \Delta t \cdot \left[(C_1 + K_1 + K_5) \cdot C_{blood_{Sev}}(t) \right] + \Delta t \cdot \left[K_2 \cdot C_{HPT_{Sev}}(t) \right] \quad (1)$$

$$C_{HPT_{Sev}}(t+\Delta t) = C_{HPT_{Sev}}(t) + \Delta t \cdot \left[K_1 \cdot C_{blood_{Sev}}(t) + K_4 \cdot C_{PPT_{Sev}}(t) \right] - \Delta t \cdot \left[(K_3 + K_2) \cdot C_{HPT_{Sev}}(t) \right] \quad (2)$$

$$C_{PPT_{Sev}}(t+\Delta t) = C_{PPT_{Sev}}(t) + \Delta t \cdot \left[K_3 \cdot C_{HPT_{Sev}}(t) - K_4 \cdot C_{PPT_{Sev}}(t) \right] \quad (3)$$

$$C_{blood_{HFIP}}(t+\Delta t) = C_{blood_{HFIP}}(t) + \Delta t \cdot \left[K_5 \cdot C_{blood_{Sev}}(t) + K_7 \cdot C_{HPT_{HFIP}}(t) \right] - \Delta t \cdot \left[(K_6 + C_2 + C_3) \cdot C_{blood_{HFIP}}(t) \right] \quad (4)$$

$$C_{HPT_{HFIP}}(t+\Delta t) = C_{HPT_{HFIP}}(t) + \Delta t \cdot \left[K_6 \cdot C_{blood_{HFIP}}(t) - K_7 \cdot C_{HPT_{HFIP}}(t)\right] \quad (5)$$

Subsequently, under the assumptions that breath concentrations are proportional (via blood/breath coefficients) to blood concentrations, we calculate:

$$C_{Breath_{Sev}}(t) = 0.65 \cdot C_{blood_{Sev}}(t) \quad (6)$$

and

$$C_{Breath_{HFIP}}(t) = 6.0 \cdot C_{blood_{HFIP}}(t) \quad (7)$$

where the C(t)'s denote concentrations, the subscripts identify the compartments and the compounds, C_a represents the concentration of SEV in the anesthetic mixture and the K_i's and C_i's denote time constants as described in the previous section. The equations can be quickly implemented using a spreadsheet software. The blood/breath partition estimates (eq. 6 and 7) are linear functions and so any uncertainty is adjusted during the model fine-tuning procedure through the adjustment of a single scaling parameter.

2.5 Methods for estimating initial parameters

The incremental equations are quantified using reasonable estimates for rate parameters that are then adjusted to fit over the empirical data. Typically, the first step is to estimate the initial uptake rate parameter (Ca · Ko) using eq. 1 above. The initial conditions are that concentrations throughout the body are zero at time = 0 and we rearrange the equation setting $C_{bloodSev}(t)$ and $C_{HPTSev}(t)$ to be very close to zero, and solve for an estimate of the initial slope:

$$C_a \cdot K_0 \approx \left[C_{blood_{Sev}}(t+\Delta t) - C_{blood_{Sev}}(t)\right] / \Delta t \quad (8)$$

which can be empirically evaluated using the earliest (uptake) data points available. Given this initial estimate for the uptake parameter and an empirical estimate for the steady state concentration from data observation, we can estimate the initial half-life in the 1st compartment using a re-arrangement of equation 1 from above and the understanding that the slope of the curve is zero:

$$\left[C_{blood_{Sev}}(t+\Delta t) - C_{blood_{Sev}}(t)\right] / \Delta t = 0 = (C_a \cdot K_0) - \left[\left(C_1 + K_1 + K_5\right) \cdot C_{blood_{Sev}}(t)\right] + \left[K_2 \cdot C_{HPT_{Sev}}(t)\right] \quad (9)$$

and therefore:

$$(C_a \cdot K_0) = \left[\left(C_1 + K_1 + K_5\right) \cdot C_{blood_{Sev}}(t)\right] - \left[K_2 \cdot C_{HPT_{Sev}}(t)\right] \quad (10)$$

This is further reduced with the assumption that $[K_1 \cdot C_{bloodSev}(t)] \approx [K_2 \cdot C_{HPTSev}(t)]$ at steady state conditions leaving the approximation:

$$(C_1 + K_5) \approx (C_a \cdot K_0) / C_{bloodSev}(t = ss) \quad (11)$$

where $C_{bloodSev}(t=ss)$ is the steady state concentration and (Ca · Ko) has been estimated in eq. 8.

Starting with these basic estimates from empirical data, we can construct the initial model and then empirically refine it with trial and error for the 2nd and 3rd compartments as well as the metabolite parameters. Initially, kinetic parameters are adjusted for the 2nd compartment to fit the curvature of the elimination at 100 to 200 minutes; subsequently, the 3rd compartment kinetic parameters are adjusted to fit the behavior past 200 minutes.

2.6 Chemical reagents

1,1,1,3,3,3-hexafluoro-2-propanol (puriss p.a. standard for GC grade > 99%) was purchased from Fluka, Sigma-Aldrich (Italy). SEV was from Abbott, Italy. Analytes were stored at 4 °C to minimize the risk of evaporation. Labelled toluene-D8 (purity 99.8 %) was purchased from ARMAR Chemicals (Switzerland).

2.7 Preparation of standards

A gaseous standard of SEV and HFIP was prepared by evaporating 5 µL of both liquids in a pre-evacuated glass flask (2 L) equipped with a septum and held at 40 °C. The corresponding concentrations were 480 ppmv for SEV and 610 ppmv for HFIP. Calibration curves for these compounds were obtained by transferring different volumes of the standard into sampling bags, and analysing the bag contents as they were breath samples.

A further gaseous standard of labelled toluene-D8 was prepared in another glass flask as described above, the corresponding concentration was 600 ppmv.

2.8 Breath sample collection

Disposable bags (approximate volume 5 L) were fabricated from a roll of Nalophan tube (polyethylene terephthalate film, thickness 20 µm) supplied from Kalle (Wiesbaden, Germany). One end of each paring was rolled and tightened by nylon cable ties, whereas the other end was wrapped and tightened around a PTFE tube connected to a stopcock, a one-way valve, and a mouthpiece. Each subject was asked to calmly fill a bag with multiple deep breaths.

2.9 Breath sample analysis

Stability tests were performed by filling Nalophan bags with standard mixtures. Results indicate that SEV concentrations were stable for 6 hours and decreased about 10% after 24 hours [28]. Sample analysis was started as soon as possible within two hours from sampling. Breath samples were collected at room temperature and then sampling bags were stabilized at 40 (±1) °C in a thermostated box for half an hour to prevent water condensation before loading a sample aliquot (250 mL) on the desorption tube. This aliquot was flowed through a drying tube filled with 9 g of anhydrous sodium sulphate for water removal, and a glass thermal desorption tube prepacked with 250 mg of Tenax GR (70% Tenax TA, 2,6-diphenyl-p-phenylene oxide and 30% graphitized carbon). During the sample transfer, the sampling bag and the drying tube were kept at 40 °C, whereas the desorption tube was at ambient temperature. Due to the high concentrations of SEV, only 50 mL of the samples collected in the first two days after surgery were transferred into the tube. The sample flow through the tubes (50 mL/min normally, 20 mL/min in the case of the early low volume samples) was regulated by the rotameter on the diaphragm pump (NMP 50, KNF). The right sampling volume was obtained by keeping the pump on for 5 minutes (2.5 minutes in the case of the early low volume samples).

The desorption tubes were thermally desorbed by an automated two-stage thermal desorption unit (STD 1000, DANI Instrument) equipped with an internal focusing trap packed with 70 mg of Tenax GR. The first desorption was carried out at 250 °C for 5 minutes under a helium splitless flow of 35 mL/min. The sample was concentrated into a 5 °C cold trap which was then rapidly heated to 250 °C. This second desorption allowed the fast transfer of the sample to a gas-chromatograph (Trace GC Ultra, Thermo Electron Corporation) equipped with a DB-624 capillary column (60 m × 0.25 mm, 1.4 µm film thickness, Agilent Technologies) and coupled to a quadrupole mass spectrometer (Trace DSQ, Thermo Electron Corporation) operated in the positive electron impact (EI) ionization (70 eV). Chromatograms were collected in both total ion current (TIC) and selected ion monitoring (SIM) acquisition modes. Column temperatures were ramped as follows: 35 °C for 10 min, 4 °C/min to 130 °C, 2 min hold, 20 °C/min to 250 °C, 10 min hold, 25 °C/min to 260 °C, 15 min hold. The inlet temperature was set at 200 °C and the GC operated at a constant pressure of 210 kPa with a split flow of 10 mL/min. Dedicated software (TDManager™, DANI Instrument; Xcalibur™, Thermo Electron Corporation) controlled the thermal desorption unit and the GC-MS.

2.10 Method evaluation

The GC/MS unit was calibrated by gaseous standards of SEV and HFIP at different concentrations that were prepared in pre-evacuated glass flasks, transferred into the sampling bags and analysed as normal samples. The system showed a good linearity ($R^2 = 0.999$) for both gases, in the ranges 0.1 – 100 ppmv and 0.002 – 0.6 ppmv for SEV and HFIP respectively. The stability of the response factor of the GC/MS

unit was checked daily by the injection of a labelled standard (toluene-D8, 99.8% purity, Armar Chemicals). The limit of detection (LOD) was calculated by the software of the instrument as the concentration giving a signal with a signal-to-noise ratio of 3, and resulted 5 and 10 pptv for SEV and HFIP, respectively. The precision of the method was assessed by repeatability and reproducibility at a concentration level of 0.5 ppmv of both compounds and expressed as coefficient of variation. The coefficients of variation were calculated based on quintuplicate runs, analysed on the same day for repeatability and on different days for reproducibility. Within run and between run precision of the method resulted 3 and 10 %, respectively. The analytical recovery was estimated for SEV and HFIP by comparing the results of replicate analyses of a bag and the analyses of desorption tubes loaded with 1 μL of each liquid. This Nalophan bag (2.5 L) was prepared by injecting 10 μL of liquid SEV and HFIP in the flow of pure air during the filling, and its content was analyzed by loading 250 mL aliquots into desorption tubes. In these conditions, the recovery of the analytes was 93% and 95% respectively.

2.11 Human subjects

Time dependent post-operative breath samples were collected from six patients undergoing various surgeries. Research was conducted under approved Institutional Review protocols with informed consent. Table 3 provides summary information for the patients including host factors (age, height, weight, gender), type of surgery, duration of surgery, and total dose of anesthetic. Figure 2 shows, as an example, the extracted ion chromatogram of a breath sample collected 216 hours after surgery from patient 3 at m/z 131 (SEV) and m/z 99 (HFIP).

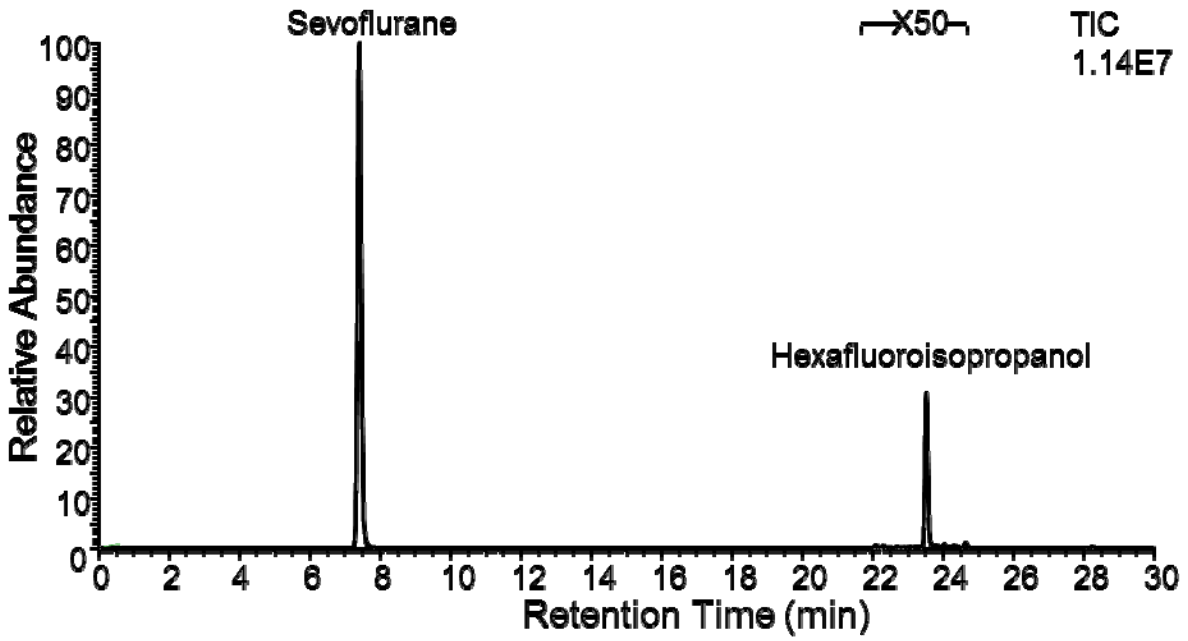

Figure 2. Extracted ion chromatogram of a breath sample collected 216 hours after surgery from patient 3 at m/z 131 (SEV, RT = 7.39 min) and m/z 99 (HFIP, RT = 23.51 min).

Table 3. Summary information concerning the patients.

Demographic data

ID	Gender	Age	Height (m)	Body weight (Kg)	Body Mass Index (Kg/m^2)
1	M	73	1.68	80	28
2	F	67	1.63	53	20
3	F	69	1.65	77	28

4	F	72	1.64	75	28
5	M	73	1.70	80	28
6	M	74	1.77	92	29

Clinical data

ID	Type of surgery	SEV			
		Duration of surgery (h)	Estimated total dose (g)	Dose by weight (mg/kg)	Dose over time (g/h)
1	Descending colectomy	3	18.9	236	6.3
2	Distal pancreatectomy	2.7	19.0	358	7.0
3	Adrenalectomy and splenectomy	4.1	10.8	140	2.6
4	Bowel resection with colostomy	6.3	41.1	548	6.5
5	Gastrectomy	4.4	34.1	423	7.8
6	Lower anterior resection	8.7	78.4	852	9.0

2.11 Breath measurement data

Post-operative breath samples were collected for up to 8-days. Table 4 provides exhaled breath concentrations by patient for the two compounds. We did not have the opportunity to collect samples during or immediately after surgery as these were all critically ill patients. Total dose values are estimates based on real time measurements of administered SEV by the surgery room monitor.

Table 4. Breath concentrations of SEV and HFIP after surgery.

Time after surgery (hrs)	SEV breath concentration (ppmv)						HFIP breath concentration (ppmv)					
	Patient						Patient					
	1	2	3	4	5	6	1	2	3	4	5	6
2	27.7	74.7	60.1	48.8	64.7	50.5	0.095	0.103	0.144	0.053	0.104	0.100

17	7.5	5.6	9.4	10.0	6.1	15.6	0.084	0.044	0.105	0.083	0.040	0.225
24	5.3	3.9	8.6	9.0	2.9	10.0	0.093	0.019	0.094	0.089	0.028	0.260
41	2.6	3.1	3.9	4.1	2.1	3.7	0.054	0.007	0.069	0.051	0.017	0.240
48	2.8	4.4	4.5	3.7	2.4	5.9	0.036	0.008	0.067	0.048	0.011	0.267
65	1.6	3.0	3.2		1.0		0.015	0.005	0.037		0.005	0.167
72	1.9			2.8		3.1	0.014			0.034		
89	1.2			2.6			0.006			0.024		
96					0.9	3.0					0.003	0.121
113	0.7	0.5	1.8	2.3			0.003	0.002	0.009	0.020		
137	0.6	0.3		1.0		0.5	0.002	0.001		0.008		0.016
144			1.3		0.4				0.004		0.001	
185				0.8						0.005		
216			0.4		0.4				0.002		0.001	

3. Results

3.1 Initial model construction

The ppmv estimated data from Kharasch et al. was used to develop the SEV and HFIP incremental models using the approach presented in the methods section. The initial estimate for SEV uptake (Ca+Ko) is 2482 ppm/min, the steady state concentration estimate in exhaled breath is 26,062 ppmv, and the initial elimination rate estimate (C1+K5) is 0.0952. Subsequently, higher compartments were empirically fitted and initial estimates were modified to account for approximations. Figure 2 (a) shows data overlaid onto the model. The two-compartment HFIP data were subsequently modeled by trial and error, and the data vs. model comparison is shown in figure 2 (b). We see that both models represent the respective data sets well over a long time frame. There is a great variability in the HFIP measurements early in the post-anesthesia period and so the model was fitted among these points and may not necessarily represent any specific individual. We have subsequently modeled the higher and lower data points separately to bracket the behavior in the first 500 minutes after the end of anesthesia (dashed curves, figure 2 (b)). This was accomplished empirically by adjusting the K_5 and $C_2 + C_3$ parameters that govern HFIP kinetics at the individual level. We interpret this envelope to indicate the between-subject variability in HFIP metabolism, and possibly differences in phase-2 glucuronidation. The final results of the model

parameters for the Kharasch data are given in table 5. Adjustments for the bracketing of HFIP response are given in table 6.

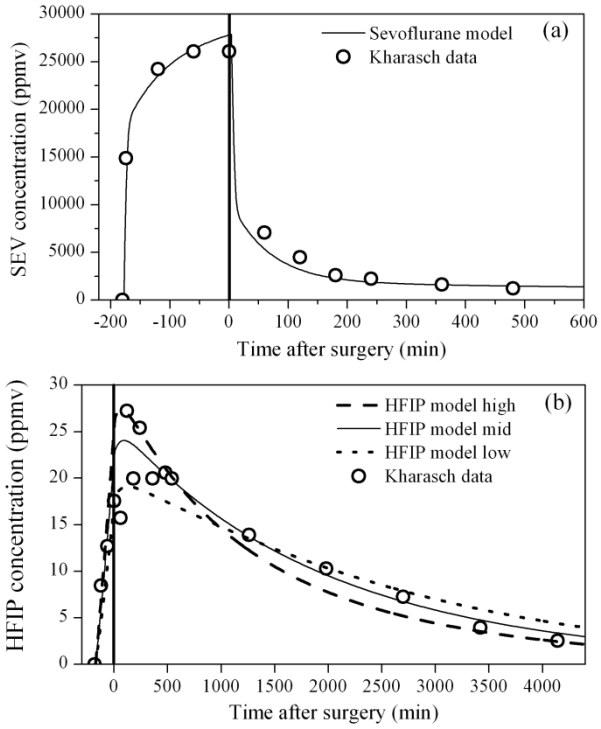

Figure 3. Empirical breath data from Kharasch et al.. 3hr anesthesia of 6 subjects overlaid onto fitted incremental models; (a) SEV in exhaled breath in ppmv and (b) HFIP metabolite in exhaled breath in ppmv; three models are presented showing data capture at high, medium, and low fits. Time scales (x-axes) are set to accommodate available data; the vertical line inserted at t=0 indicates the end of anesthesia.

Table 5. Parameters for SEV and HFIP models based on Kharasch data.

Compound	Parameter	Description	Value
SEV	Ko	SEV blood uptake	3100
	C1	SEV blood elimination	0.105
	K1	SEV from blood to HPT	0.055
	K2	SEV from HPT to blood	0.018

	K3	SEV from HPT to PPT	0.004
	K4	SEV from PPT to HPT	0.0017
HFIP	K5	HFIP production	5.50E-06
	C2+C3	HFIP loss	9.00E-04
	K6	HFIP from blood to HPT	9.00E-06
	K7	HFIP from HPT to blood	2.00E-06

Table 6. Standard parameters for inter-individual variability for HFIP models and necessary adjustments from original Kharasch model in Table 5.

HFIP Model	**K5 (1/min)**	**C2 +C3 (1/min)**	**Time delay (min)**
Kharasch (low)	3.58E-06	7.20E-04	na
Kharasch (mid)	5.50E-06	9.00E-04	na
Kharasch (high)	7.15E-06	1.17E-03	na
Patient 1	4.95E-06	9.00E-04	na
Patient 2	5.50E-06	1.80E-03	na
Patient 3	4.40E-06	8.10E-04	na
Patient 4	9.08E-06	9.90E-04	355
Patient 5	6.05E-06	1.80E-03	na
Patient 6	1.43E-06	6.30E-04	520

3.2 Model application/validation: Yasuda data

To test the assumption that the SEV model (and by inference, the HFIP model) are both subject to linear kinetics, we apply the existing model from above to the completely independent data from Yasuda et al.. The only adjustment is for the different administered SEV concentration (10,000 ppmv) and shorter administration time (30 min). The model slightly under-predicts speed of uptake and speed of elimination (figure 3). We attribute this apparent higher pulmonary efficiency to the pre-selection of healthy young subjects (mean age 23 yrs) and the fact that they did not undergo invasive surgery. In contrast, the Kharasch's patients used to build the model all had invasive, albeit elective surgery and ranged from 23 to 68 yrs. in age.

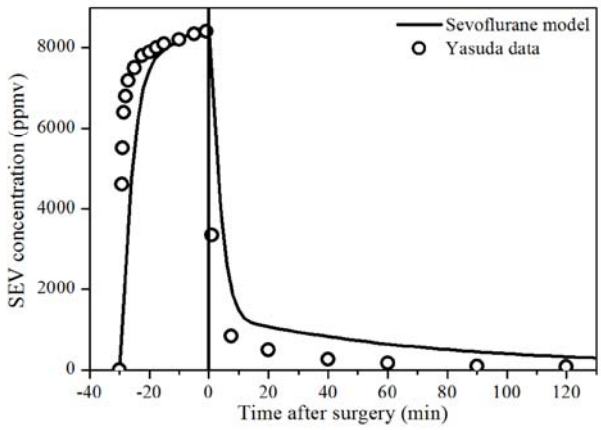

Figure 4. Original model (based on Kharasch data) is applied to directly to SEV data from table 2 (Yasuda). The model slightly under-predicts speed of uptake and speed of elimination, but overall shape and levels are consistent. This is expected, as the Yasuda subjects were young, healthy volunteers (mean age 23 ± 3 yrs) without surgical intervention in contrast to the Kharasch patients that were appreciably older (mean age 44 ± 4 yrs) and undergoing invasive, albeit elective, surgery.

3.3 Model application: Pisa Surgical Data

Under the assumptions of linearity of classical PK, we used the fitted rate constants from the model development data (Kharasch) and applied the empirical model directly to the measurements (and time meta-data) made for six patients (tables 3 and 4). The only adjustment made was to calibrate the initial condition at t=0 for the SEV model for each individual as they all had different lengths of surgeries and different administered levels of anesthetic; the HFIP model parameters were left identical to the initial models shown in figure 2 (b) as the metabolism calculation is only dependent on SEV concentration.

In contrast to the excellent performance of the incremental PK model for SEV shown in figure 4, the results for the empirical HFIP data are somewhat erratic. In figure 5 (a) we observe that four of the six patients (#'s 1, 2, 3, and 5) had the expected biologically damped elimination response, although the model tended to over-predict the production of HFIP in a range from 10% to 50%; Patients #4 and #6, however, exhibited an anomalous HFIP response. Rather than the expected damped exponential elimination, they both increased over time for 24 and 48 hours, respectively. Figure 5 (b) shows the empirical measurements, the expected PK behavior, and an empirical sketch that required a polynomial to approximate the actual shape.

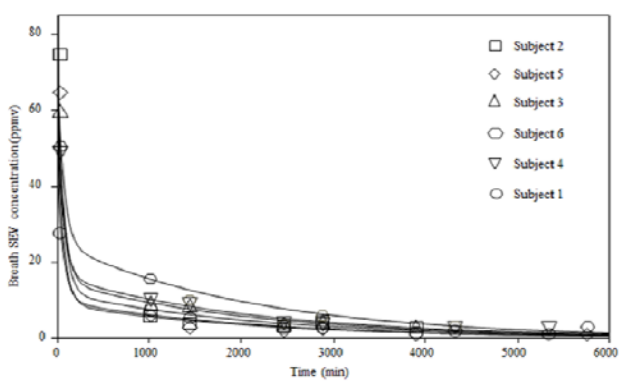

Figure 5. PK model for SEV applied to Pisa study of six patients undergoing invasive surgeries with SEV anesthesia. The model is robust and accurately fits breath uptake and elimination on an individual basis requiring only a single parameter calibration proportional to administered dose and length of surgery.

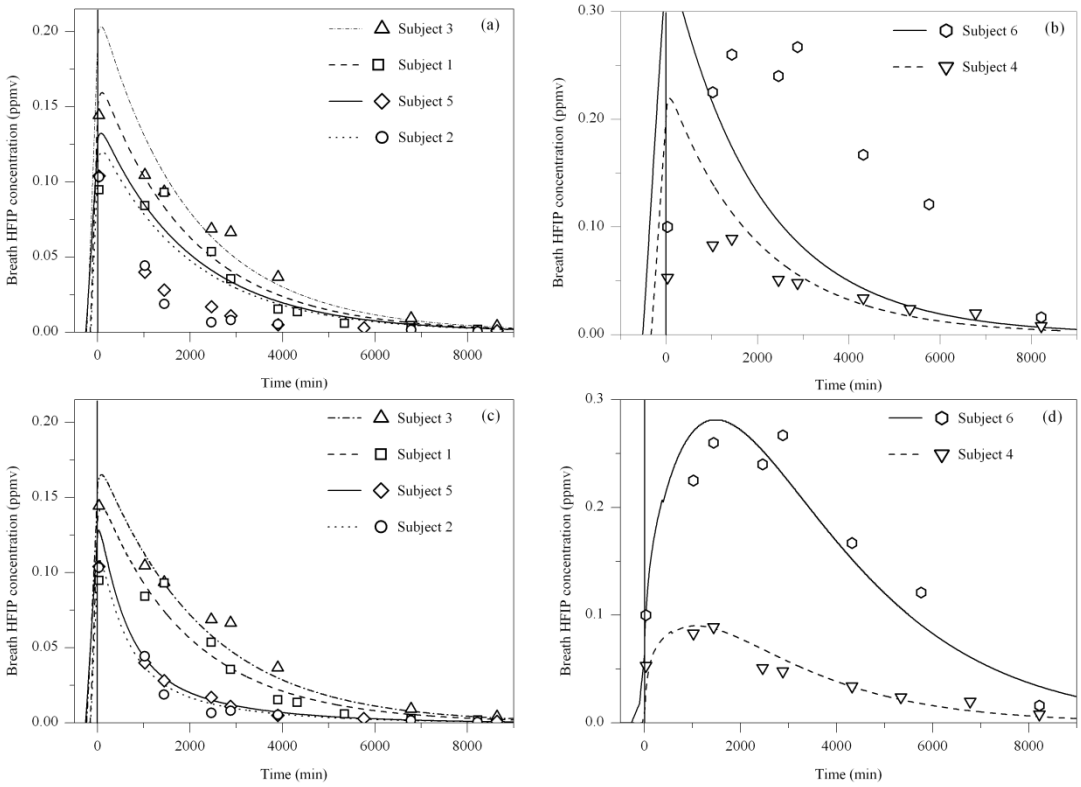

Figure 6. PK model for HFIP: subjects with the expected biological damped elimination behavior (1, 2, 3, 5) (a) and with anomalous behavior (4, 6) (b). The model can be customized to reflect individual metabolic parameters: patients 1, 2, 3, and 5 (c), patients 4 and 6 (d), wherein a delay in metabolism was introduced.

The depression of response with respect to the model based on Kharasch data for subjects 1, 2, 3, and 5 (figure 5 (a)) can be interpreted as lower efficiency of CYP2E1 function in the liver. This is not surprising as the model is based on moderately healthy patients undergoing elective surgery (Kharasch 1991), whereas the subjects of this study were older and less healthy having very invasive life-saving surgeries.

For this reason, we recalculated the HFIP response for these initial four subjects by decreasing the rate of HFIP formation in 5% steps below that of the mean value from the Kharasch based model. We found that this gives a better model approximation, but still did not fully explain the shape of the curve. We then further adjusted the loss parameter of HFIP from the blood; this is a composite of the efficiency of ventilation and the relative amount of removal via glucuronidation achieving a predictive model that now fits empirical measurements.

For subjects 4 and 6, the interpretation is more difficult; there appears to be a time delay in production of HFIP in addition to rate differences (recall figure 5 (b)). The adjusted parameters for all subjects are contrasted to the nominal central model and the bracketed models for HFIP previously shown (figure 2 (b)). The final results are given in table 6 wherein we see that adjustments are essentially within the band of the original Kharasch model. Figures 5 (c) and (d) reflect the adjusted models for the individual subjects.

The apparent delay (and reduction) in HFIP production is significant in a number of ways. First, it may be a non-invasive assessment of overall liver function due to surgical trauma or possibly due to needed repair functions that could overwhelm or saturate the CYP2E1 metabolism of SEV. Second, it could be used eventually as an indicator of return to function after transplantation and reperfusion. The models could easily be calibrated (as they were for subjects 4 and 6) to assess such parameters. From an environmental exposure standpoint, SEV could conceivably be used as a probe molecule at low levels to assess population based liver function in various urban, suburban, and rural environments.

4. Discussion

The implementation of a simple iterative PK model shown that the kinetics and metabolism of a tracer compound (SEV) can be explored in a general manner from literature values. The model was applied to a new set of observations from different patients under the assumptions of linear kinetics to predict blood- and breath-borne SEV concentrations. Subsequently, we developed an incremental model that calculates the production of HFIP, the primary metabolite of SEV, under the assumption of normal (nominally healthy) metabolism. We proposed that monitoring HFIP simultaneously with SEV tracer compound is a direct link to CYP2E1 metabolism, and as such, deviations from expected HFIP production is a marker for liver function efficiency.

We conclude that SEV is an excellent probe chemical for liver function as it is used routinely in human surgery and poses little if any chemical risk. Although there is a fair amount of between subject variance as discussed regarding the nominally healthy Kharasch sample cohort above, the appearance of *any* HFIP in blood and breath only occurs through liver metabolism. As such, real-time monitoring of HFIP could serve as an immediate indication of re-established liver function during transplant surgery. Furthermore, below-anesthetic doses of SEV could be used to monitor liver metabolism rates in out-patient or public health applications, or be used as a probe chemical for *in vitro* studies of chemical toxicity in human cell lines.

Acknowledgements

The authors thank Jon Sobus, Tzipporah Kormos, Michael Madden, Andrew Ghio, Elin Ulrich, and Myriam Medina-Vera of US EPA for their expert advice. This research has been subjected to (EPA) Agency review and approved for publication. Mention of trade names or commercial products does not constitute endorsement or recommendation for use.

References

[1] Hoekstra L T, de Graaf W, Nibourg G A A, Heger M, Bennink R J, Stieger B and van Gulik T M 2013 Physiological and Biochemical Basis of Clinical Liver Function Tests. A Review *Annals of Surgery* **257** 27-36

[2] Burra P and Masier A 2004 Dynamic tests to study liver function *European review for medical and pharmacological sciences* **8** 19-21

[3] Freeman R B, Dixon M, Horth B, Melanson A M, Palladino M B, Kinzel J, Rohrer R, Cooper J, Reid J and Modak A S 2007 L-[1-C-13] phenylalanine breath test for monitoring hepatic function after living donor liver transplant surgery *J Breath Res.* **1** 026002

[4] Schmidt L E, Olsen A K, Rasmussen A, Kirkegaard P and Dalhoff K 2001 Early postoperative erythromycin breath test measures hepatic CYP3A4-activity and predicts graft function in liver transplant recipients *J Hepatol.* **34** 36-36

[5] Collom S L, Jamakhandi A P, Tackett A J, Radominska-Pandya A and Miller G P 2007 CYP2E1 active site residues in substrate recognition sequence 5 identified by photoaffinity labeling and homology modeling *Arch Biochem Biophys.* **459** 59–69

[6] Kharasch E D and Thummel K E 1993 Identification of cytochrome P450 2E1 as the predominant enzyme catalyzing human liver microsomal defluorination of sevoflurane, isoflurane and methoxyflurane *Anesthesiology.* **79** 795–807

[7] Yoon M, Madden M C and Barton H A 2007 Extrahepatic metabolism by CYP2E1 in PBPK modeling of lipophilic volatile organic chemicals: impacts on metabolic parameter estimation and prediction of dose metrics *J Toxicol Environ Health A.* **70** 1527–41

[8] Pleil J D, Fisher J W and Lindstrom A B 1998 Comparison of human blood and breath levels of trichloroethylene from controlled inhalation exposure *Environ Health Perspect.* **106** 573–80

[9] Pleil J D 2008 The Role of Exhaled Breath Biomarkers in Environmental Health Science *Journal of Toxicology and Environmental Health, B. Critical Reviews* **11** 613-26

[10] Lindstrom A B, Pleil J D and Berkoff D C 1997 Alveolar breath sampling and analysis to assess trihalomethane exposures during competitive swimming training *Environ Health Perspect.* **105** 636–42

[11] Tan Y M, Sobus J R, Chang D, Goldsmith M, Tornero-Velez R, Pleil J D and Dary C C 2012 Reconstructing Human Exposures Using Biomarkers of Exposure and Other Clues *Journal of Toxicology and Environmental Health, B. Critical Reviews* **15** 22-38

[12] Pleil J D, Sobus J R, Sheppard P R, Ridenour G and Witten M L 2011 Strategies for evaluating the environment-public health interaction of long-term latency disease: the quandary of the inconclusive case-control study *Chemico-Biological Interactions* **196** 89-95

[13] Pleil J D, Kim D, Prah J, Ashley D L and Rappaport S M 2007 Exposure reconstruction for reducing uncertainty in risk assessment: example using MTBE biomarkers and a simple pharmacokinetic model *Biomarkers.* **12** 331–48

[14] Sobus J R, Pleil J D, McClean M D, Herrick R F and Rappaport S M 2010 Biomarker variance component estimation for exposure surrogate selection and toxicokinetic inference *Toxicology Letters* **199** 247-53

[15] Kim D, Andersen M E, Pleil J D, Nylander-French L A and Prah J D 2007 Refined PBPK model of aggregate exposure to methyl tertiary-butyl ether *Toxicol Lett.* **169** 222–35

[16] Pleil J D 2012 Categorizing biomarkers of the human exposome and developing metrics for assessing environmental sustainability *Journal of Toxicology and Environmental Health, B. Critical Reviews* **15** 264-80

[17] Kharasch E D, Karol M D, Lanni C and Sawchuk R 1995 Clinical sevoflurane metabolism and disposition: I. Sevoflurane and metabolite pharmacokinetics *Anesthesiology.* **82** 1369–78

[18] Yasuda N, Lockhart S H, Eger E I II, Weiskopf R B, Liu J, Laster M, Taheri S and Peterson N A 1991 Comparison of kinetics of sevoflurane and isoflurane in humans *Anesth Analg.* **72** 316–24

[19] Patel S S and Goa K L 1996 Sevoflurane: a review of its pharmacodynamic and pharmacokinetic properties and its clinical use in general anaesthesia *Drugs.* **51** 658–700

[20] Belda J F, Soro M, Badenes R, Meiser A, Garcia M L, Aguilar G and Marti F J The predictive performance of a pharmacokinetic model for manually adjusted infusion of liquid sevofluorane for use with the Anesthetic-Conserving Device (AnaConDa): A clinical study *Anesthesia and Analgesia* **106** 1207-14

[21] Holaday D A and Smith F R 1981 Clinical characteristics and biotransformation of sevoflurane in healthy human volunteers *Anesthesiology.* **54** 100–6

[22] Shiraishi Y and Ikeda K 1990 Uptake and biotransformation of sevoflurane in humans: a comparative study of sevoflurane with halothane, enflurane, and isoflurane *J Clin Anesth.* **2** 381–6

[23] Kharasch E D 1995 Biotransformation of sevoflurane *Anesth Analg.* **81** S27-38

[24] Kharasch E D, Armstrong A S, Gunn K, Artru A, Cox K and Karol M D 1995 Clinical sevoflurane metabolism and disposition: II. The role of cytochrome P450 2E1 in fluoride and hexafluoroisopropanol formation *Anesthesiology.* **82** 1379–88

[25] Pleil J D and Sheldon L S 2011 Adapting concepts from systems biology to develop systems exposure event networks for exposure science research *Biomarkers.* **16** 99–105

[26] Edwards S W and Preston R J 2008 Forum: systems biology and mode of action based risk assessment *Toxicol Sci.* **106** 312–8

[27] Bourdeaux D, Sautou-Miranda V, Montagner A, Perbet S, Constantin J M, Bazin J E and Chopineau J 2010 Simple assay of plasma sevoflurane and its metabolite hexafluoroisopropanol by headspace GC–MS *J Chromatogr B* **878** 45–50

[28] Ghimenti S. 2011 Chemical information from human fluids for therapy monitoring and clinical diagnosis *PhD Thesis in Chemical Science, University of Pisa* 200.